FULL LENGTH ARTICLE

Chondroitin Polymerizing Factor (CHPF) promotes cell proliferation and tumor growth in human osteosarcoma by inhibiting SKP2's ubiquitination while activating the AKT pathway

Yi Shen [a], Jun Li [a], Dan Peng [a], Lele Liao [a], Xia Chen [a], Weiye Zhong [a], Zicheng Liu [a], Chao Yu [a], Yuanliang Sun [b],*

[a] Department of Orthopaedics, The Second Xiangya Hospital of Central South University, Changsha, Hunan 410000, China
[b] Department of Spine Surgery, Affiliated Hospital of Qingdao University, Qingdao, Shandong 266000, China

Abstract Osteosarcoma is a common malignant tumor occurring in children and young adults. Chondroitin sulfate (CS) participates in cell adhesion, cell division, and the formation of neural networks in the body, the biosynthesis of which requires the participation of glycosyltransferases. CHPF, a glycosyltransferase, plays a role in the extension of CS. Recently, CHPF's biological roles and functional importance in human diseases including malignant tumors have been widely discussed. However, whether CHPF is involved in osteosarcoma development and growth has not been revealed. The present work aimed to investigate the expression levels, functional significance and molecular mechanism of CHPF in osteosarcoma progression. Our results revealed that CHPF is strongly expressed in osteosarcoma tissues and cells. Furthermore, CHPF serves as a tumor promoter in the development and progression of osteosarcoma through enhancing cell proliferation and migration while suppressing apoptosis. Exploration of the mechanism by which CHPF promotes osteosarcoma indicated that CHPF promotes osteosarcoma through counteracting SKP2's ubiquitination and activating the Akt signaling pathway.

---

* Corresponding author. Department of Spine Surgery, Affiliated Hospital of Qingdao University, NO.16 jiangsu road Qingdao city, Qingdao, Shandong 266000, China.
E-mail address: sunyuanliang@qduhospital.cn (Y. Sun).

Introduction

Osteosarcoma, a common malignant tumor occurring in children and young adults, is classified into several sub-types and characterized by a high risk of metastasis progression and recurrence after treatment.[1] The current treatments for osteosarcoma include combined surgery and neoadjuvant chemotherapy drugs. Despite great advancements in the treatment methods, the overall survival of patients with osteosarcoma remains unsatisfactory.[2] Thus, there is an urgent need to study the molecular targets and related signaling pathways that modulate osteosarcoma in order to determine novel targets for osteosarcoma treatment.

Chondroitin sulfate (CS), a polysaccharide composed of a variety of alternating sugars (such as N-acetylgalactosamine and glucuronic acid), participates in cell adhesion, cell division, and the formation of neural networks in the body.[3,4] The biosynthesis of CS requires the participation of glycosyltransferases.[5] One of the identified glycosyltransferases, chondroitin polymerizing factor (CHPF), mainly affects the extension of CS.[6] CHPF, a 775 amino acid type II transmembrane protein, is located in the 2q35-q36 region of the human chromosome, spanning four exon regions.[7−9] Recently, CHPF's biological functions and roles in human diseases have been widely discussed. For example, Takeuchi et al investigated the correlation between the content of individual glycosaminoglycans and the histological patterns in breast tumor tissues, suggesting that myxomatous stroma of intracanalicular fibroadenoma contained a large amount of glycosaminoglycans and the chondroitin 4- and 6-sulfate.[10] In addition, a study from Pothacharoen et al indicated that the loss of chondroitin sulfate-proteoglycans (CS-PGs) is a frequent event in osteoarthritis.[11] Moreover, in patients suffering from neuropathy, the average length of chondroitin chains formed on the non-reducing terminal GalNAc(4S)-linkage structure by complexes comprising ChSy-1 F362S and CHPF, ChSy-2, or ChSy-3 was much shorter than that formed by the wild-type complexes, which implied that the progression of peripheral neuropathies may result from defects in these regulatory systems.[12] On the other hand, some publications have reported the relationship between CHPF and human cancers including colorectal cancer,[13] laryngeal cancer,[14] and glioma,[15] indicating that CHPF overexpression is strongly related to the occurrence and development of tumors. However, the expression levels and functional importance of CHPF in the development and outgrowth of osteosarcoma have not been studied in detail.

In this work, we revealed that CHPF serves as a tumor promoter in the development and progression of osteosarcoma, while depletion of CHPF suppressed the malignant progression of osteosarcoma. Further investigation suggested that the underlying mechanism by which CHPF promotes osteosarcoma is through the regulation of SKP2 and the Akt signaling pathway. To our knowledge, this is the first study to clarify the roles of CHPF in osteosarcoma development, which may represent a novel therapeutic target in treatment strategies for osteosarcoma.

Materials and methods

Tissue specimens and cell lines

The tissue microarray (TMA, Cat. No. OS804c), containing 79 osteosarcoma tissues and 20 para-carcinoma tissues, was provided by Xi'an Alenabio Co., Ltd. (Xi'an, China) (http://www.alenabio.com/tissue-array/Lung/LC6161). All the patients signed an informed consent form before providing samples. This research received ethical support from the Animal Care Committee of The Second Xiangya Hospital of Central South University.

Three human osteosarcoma cell lines, SAOS-2, U-2OS, and MNNG/HOS, were purchased from the Cell Resource Center, Institute of Basic Medicine, Chinese Academy of Medical Sciences (Beijing, China). The media corresponding to the above cells were McCoy's5A + 10% fetal bovine serum (FBS), 1640 + 10% FBS, and MEM + 10% FBS, respectively. The cells were placed in a 37 °C incubator containing 5% CO_2 for incubation.

Immunohistochemistry (IHC)

The samples were deparaffinized with xylene three times, followed by washing with alcohol (China National Pharmaceutical Group Co., Ltd, Beijing, China). Next, the slides were repaired with 1 × EDTA (Beyotime Biotechnology Co., Ltd, Shanghai, China) and blocked with 3% H_2O_2 and 5% goat serum (Hengyuan Biotechnology Co., Ltd, Shanghai, China). Primary antibodies (CHPF, SKP2, and Ki-67) were added and incubated at 4 °C overnight. Afterwards, the slides were washed 3 times (5 min/time) with 1 × PBST buffer. Subsequently, secondary antibodies were added, incubated and washed as described above. The slides were then stained with DAB and hematoxylin (Baso Diagnostics Inc., Zhuhai, China), and neutral resin (China National Pharmaceutical Group Co., Ltd, Beijing, China) was used to seal the samples before analyzing under an optical microscope (IX73, Olympus). The images were assessed as negative (0), positive (1−4), ++ positive (5−8), or +++ positive (9−12), with reference to the sum of the staining intensity (varied from weak to strong) and staining extent scores, which were graded as 0 (0%), 1 (1%−25%), 2 (26%−50%), 3 (51%−75%), or 4 (76%−100%). The antibodies used in this section were listed in Table S1.

Plasmid construction and lentivirus infection

For RNA interference lentiviral vectors, using CHPF, SKP2, CCND2, CCNE2, or RHOU as templates, we designed RNA interference target sequences (shCHPF: AGCTGGCCATGC-TACTCTTTG; shSKP2: AAACTCAAATTTAGTGCGACT; shCC ND2: TCGGAGGATGAACTGGACCAA; shCCNE2: GAGCAGA-TATGTTCATGACAA; and shRHOU: TTCCAGAACGTCAGTGA-GAAA). These sequences were inserted into the BR-V-108 vector through the restriction sites at both ends and transformed into TOP 10 E. coli competent cells (Tiangen, Beijing, China). Additionally, to overexpress CHPF, we designed primer amplification sequences (F-5′-3′: AGGTC-GACTCTAGAGGATCCCGCCACCATGCGGGCATCGCTGCTGCGT C, R-5′-3′: TCCTTGTAGTCCATACCGGTGCTGTTGCCCTGCTCC TGTTC) using CHPF as a template to construct a CHPF overexpression lentiviral vector. The plasmids of positive recombinants were extracted with the EndoFree maxi plasmid kit (Tiangen, Beijing, China), and the concentration was determined in a spectrophotometer (Thermo Nanodrop 2000).

For lentivirus infection into MNNG/HOS and U-2OS cells, cells in the logarithmic growth period were infected by adding 20 μL 1 $\times$ 10^8 TU/mL lentivirus under the condition of ENI.S + Polybrene, before culturing in MEM +10% FBS and 1640 + 10% FBS media, respectively, in a 6-well plate (2 $\times$ 10^5 cells/well). Finally, the infection efficiency was evaluated by microscopic fluorescence, and the knockdown efficiency was assessed by quantitative reverse-transcription polymerase chain reaction (qRT-PCR) and Western blot.

RNA extraction, cDNA synthesis, and qRT-PCR

The total RNA of MNNG/HOS and U-2OS cells was isolated using TRIzol reagent (Sigma, St. Louis, MO, USA) and used for cDNA synthesis and qRT-PCR using the Promega M-MLV Kit (Promega Corporation, Madison, Wisconsin, USA) and the SYBR Green Mastermix Kit (Vazyme, Nanjing, Jiangsu, China). GAPDH was used as an internal normalization control. The relative expression of mRNA was evaluated based on the $2^{-\triangle\triangle Ct}$ method. The primer sequences (5′-3′) were listed in Table S2.

Western blot assay

MNNG/HOS and U-2OS cells were collected after infection with lentivirus or SC79 (an AKT activator) treatment and lysed with 1 $\times$ Lysis Buffer lysis (Cell Signal Technology, Danvers, MA) to harvest protein. The protein purity was quantified using the BCA method. Next, 10% SDS-PAGE was used to segregate total protein before transferring to PVDF membranes. The membranes were blocked in TBST solution with 5% non-fat milk and subsequently incubated with primary antibodies at 4 °C overnight. After that, the membranes were washed 3 times (10 min/time) with TBST solution. Subsequently, the membranes were incubated using secondary antibodies at room temperature (RT) for 2 h and washed as described above. Finally, the ECL + plusTM Western blotting system was used for color rendering and X-ray imaging was captured with medical X-ray film (Kodak). For the Co-

Immunoprecipitation (Co-IP) assay, proteins were immuno-precipitated with anti-Flag and anti-SKP2 and then subjected to Western blotting with CHPF and SKP2 antibodies (Table S1).

Cell proliferation detection

Cell proliferation was detected by MTT assay. Briefly, after infection with the indicated lentivirus, MNNG/HOS and U-2OS cells were collected and resuspended using Dulbecco's modification of Eagle's medium Dulbecco (DMEM, Corning). Next, 100 μL cell suspension was cultured in 96-well plates at 2,000 cells/well for 5 days. Subsequently, 100 μL DMSO was added and shaken for 2–5 min. The optical density (OD) value at 490 nm wavelength was measured with a microplate reader (Tecan infinite, Mannedorf Zurich, Switzerland).

Cell proliferation was also detected using the Celigo cell counting assay. In detail, MNNG/HOS cells with shCCND2, shCCNE2, shRHOU, or shSKP2 were collected and seeded into 96-well plates at a density of 2000 cells/well and placed in an incubator with 5% CO$_2$ at 37 °C. Images of the cells were taken by the Celigo image cytometer (Nexcelom Bioscience, Lawrence, MA, USA) and a continuous 5-day cell proliferation curve was drawn.

Colony formation assay

After infection with the indicated lentivirus, MNNG/HOS and U-2OS cells were seeded into a 6-well plate (2 mL/well) for 5 days to form colonies. Visible clones in a 6-well plate were recorded by a fluorescence microscope (Olympus, Tokyo, Japan). Finally, the cells were washed with phosphate-buffered saline (PBS), fixed with 1 mL 4% para-formaldehyde, and stained with 500 μL Giemsa (Dingguo, Shanghai, China).

Cell migration assay

Cell migration was investigated using a Transwell assay. Specifically, after infection with the indicated lentivirus, MNNG/HOS and U-2OS cells were cultured to adjust the density of cells to 1 $\times$ 10^5 cells/mL, before loading into the chamber of the Corning Transwell Kit (Corning, Inc., Corning, NY, USA) containing serum-free medium. Then, the chamber was transferred to the lower chamber with 30% FBS and incubated for 72 h. Finally, 400 μL Giemsa was used for cell staining and the cell migration ability was quantified.

We next performed a wound-healing assay. Briefly, after infection with the indicated lentivirus, MNNG/HOS and U-2OS cells were seeded in a 96-well plate (5 $\times$ 10^4 cells/well). Then, the cells were incubated in an incubator with 5% CO$_2$ at 37 °C and observed under a microscope at 8 h and 24 h. The experiment was repeated three times and the migration rate of cells was evaluated based on the scratch images.

Flow cytometry assay

To investigate apoptosis, lentivirus-infected MNNG/HOS and U-2OS cells or MNNG/HOS cells after SC79 treatment

were cultured in 6-well plates (2 mL/well) for 5 days. Next, 10 μL Annexin V-APC was added for 10—15 min at room temperature in the dark, and the level of apoptosis was measured using a FACSCalibur flow cytometer (BD Biosciences, San Jose, CA, USA).

For cell cycle analysis, the above cells were cultured in 6-well plates (5 mL/well) for 5 days. The cells were stained with cell staining solution (40 × PI, 2 mg/mL: 100 × RNase, 10 mg/mL: 1 × PBS = 25:10:1,000) for 30 min. The percentage of cells in the G0-G1, S, and G2-M phases were evaluated and compared.

Human apoptosis antibody array

The effects of CHPF depletion on the apoptosis-related protein expression were detected in MNNG/HOS cells using the Human Apoptosis Antibody Array. Following cell lysis, the Handling Array membranes were blocked in 2 mL 1 × Wash Buffer II and incubated with cell lysates and 1 × Biotin-conjugated Anti-Cytokines overnight at 4 °C. Finally, the signals of the membranes were tracked using a chemiluminescence imaging system.

PrimeView human gene expression array

Total RNA was extracted as described previously. The quality and integrity of RNA were determined by a Nanodrop 2000 (Thremo Fisher Scientific, Waltham, MA, USA) and Agilent 2100 and Agilent RNA 6000 Nano Kits (Agilent, Santa Clara, CA, USA). Referring to the manufacturer's instructions, RNA sequencing was performed using Affymetrix human GeneChip PrimeView and the data were scanned by an Affymetrix Scanner 3000 (Affymetrix, Santa Clara, CA, USA). The statistical significance of the raw data was completed using a Welch t-test with Benjamini-Hochberg FDR (|fold change| $\geq$ 1.3 and FDR < 0.05 as significant). A significant difference analysis and functional analysis based on Ingenuity Pathway Analysis (IPA) (Qiagen, Hilden, Germany) were executed, and a |Z - score| > 0 is considered valuable.

Therapeutically applicable research to generate effective treatments (TARGET) database analysis

In this study, the gene expression correlation analysis was based on the RNAseq counts data (https://target-data.nci.nih.gov/Public/OS/mRNA-seq/) of 88 cases of osteosarcoma samples from TARGET (https://ocg.cancer.gov/programs/target/data-matrix).

Construction of a nude mouse tumor formation model

All animal experiments conformed to the European Parliament Directive (2010/63/EU) and were approved by the Animal Care Committee of the Second Xiangya Hospital of Central South University. Four-week-old female BALB-c nude mice (Beijing Weitong Lihua Animal Research Co., Ltd.) were used to establish a xenograft model. The mice were randomly divided into the indicated groups (n = 10),

and 4 × 10⁶ MNNG/HOS cells with shCHPF and shCtrl were resuspended in 100 μL PBS and subcutaneously injected into nude mice. The tumor volume was recorded during the entire feeding period, and 0.7% sodium pentobarbital was injected intraperitoneally for several minutes on the last day of feeding. The fluorescence was observed using an *in vivo* imaging system (IVIS Spectrum, Perkin Elmer). After 36 days, the mice were sacrificed, and the tumors were removed for weighing and photographing before freezing in liquid nitrogen and storing at −80 °C.

Analysis of protein degradation

To analyze protein degradation, MNNG/HOS cells were treated with 50 μg/mL cycloheximide (CHX) and harvested at indicated time points. The cell lysate was subjected to immunoblotting. For the analysis of protein ubiquitination of SKP2, cells were co-transfected with shCHPF and ubiquitin. At 24 h after infection, the proteasome inhibitor MG132 (10 μM) was added and the cells were incubated for 6 h. The SKP2 or IgG antibodies were added to the cell lysate before incubation overnight at 4 °C. Protein A/G Plus-agarose was added, and the mixture was incubated at 4 °C for 4 h. The ubiquitin was detected using a ubiquitin antibody. The antibodies used are detailed in Table S1.

Statistical analysis

Statistical analysis was conducted using GraphPad Prism 8 (San Diego, CA, USA) and SPSS 19.0 (IBM, SPSS, Chicago, IL, USA). All data are represented as the mean ± SD from at least three independent experiments. Student's t test (for comparisons of two groups) and one-way ANOVA (for multiple group comparisons) were used to analyze the statistical significance. Spearman's correlation analysis and Mann—Whitney U analysis were used to assess the association between CHPF expression and the pathological characteristics of osteosarcoma patients. P < 0.05 was considered significantly different. All experiments were performed in triplicate.

Results

CHPF is strongly expressed in osteosarcoma

To examine the roles played by CHPF in osteosarcoma, we first detected CHPF protein levels in osteosarcoma and para-carcinoma tissues. Of the 79 osteosarcoma samples, 52 harbored high CHPF levels (65.8%), which indicated that CHPF was more highly expressed in osteosarcoma tissues compared to para-carcinoma tissues (P < 0.001; Fig. 1A, B and Table S3). We also evaluated CHPF levels in three osteosarcoma cell lines and found high expression, especially in U-2OS and MNNG/HOS cells (Fig. 1C). Subsequently, the Mann—Whitney U analysis and Spearman's rank correlation analysis were performed to reveal the relationship between CHPF levels and clinicopathological characteristics of patients suffering from osteosarcoma. Both analyses suggested that elevated CHPF levels predicted higher-
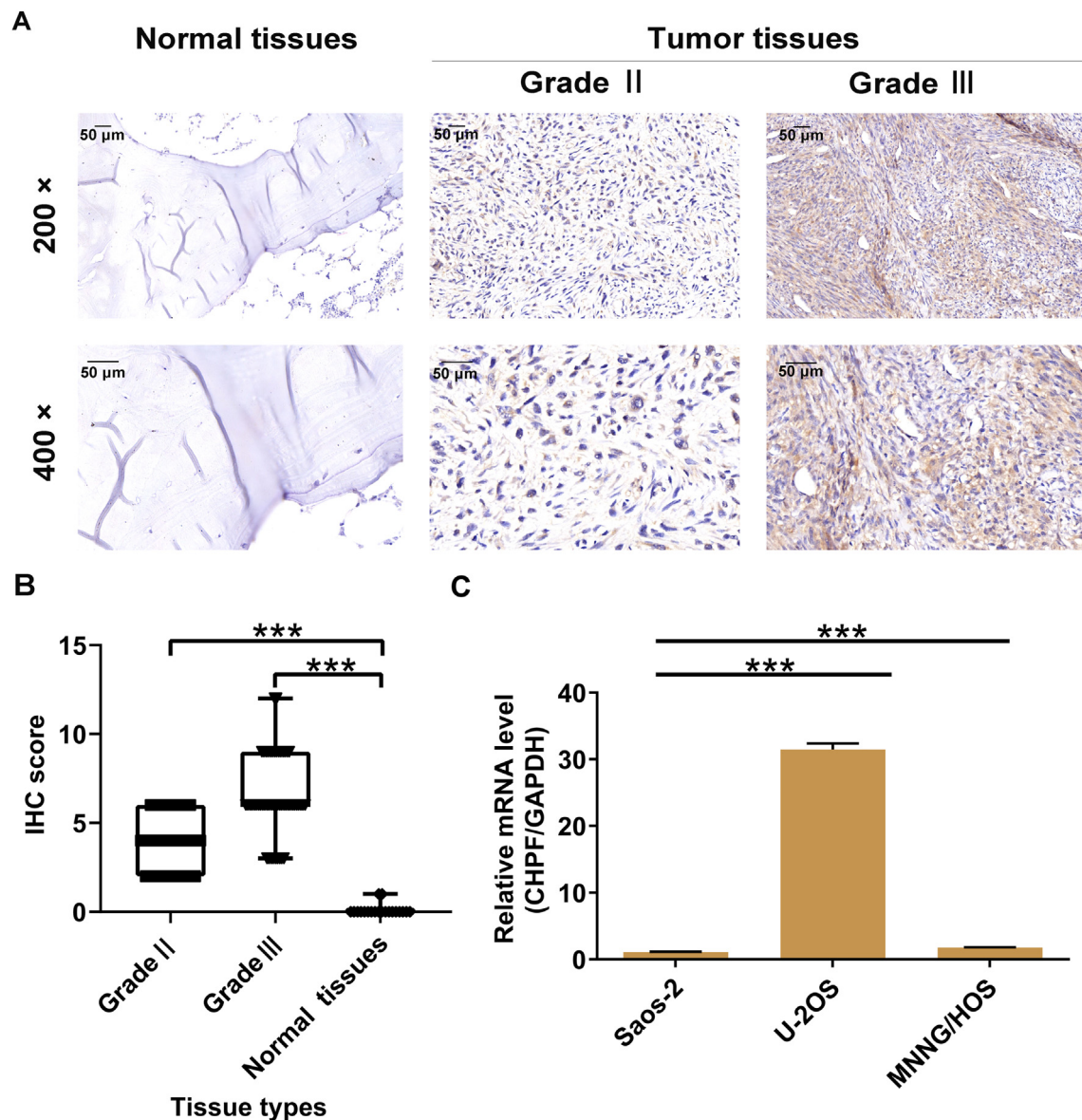
A

Figure 1 CHPF was abundantly expressed in osteosarcoma. **(A)** The protein expression of CHPF in osteosarcoma and normal tissues was detected by IHC staining. **(B)** The IHC staining score of CHPF in osteosarcoma and normal tissues was quantified. **(C)** The mRNA expression of CHPF in osteosarcoma cell lines was detected by qRT-PCR.

grade malignancy and higher pathological stage (both $P < 0.001$; Table S4, S5). Therefore, elevated expression of CHPF is likely to have significance in the progression of osteosarcoma.

CHPF knockdown blocks the development and progression of osteosarcoma *in vitro*

To further validate the functional roles of CHPF in osteosarcoma development, we knocked down CHPF in U-2OS and MNNG/HOS cells (Fig. S1), and performed MTT viability, wound-healing/Transwell migration and flow cytometry experiments. As shown in Figure 2A, the proliferation of U-2OS and MNNG/HOS cells was significantly inhibited upon silencing CHPF ($P < 0.001$), and the colony-forming ability

of both osteosarcoma cells with CHPF knockdown was restrained as well ($P < 0.001$; Fig. 2B). Besides, CHPF knockdown also obviously prevented cell migration, as assessed through Transwell and wound-healing assays ($P < 0.001$; Fig. 2C, D). Moreover, depleting CHPF caused MNNG/HOS and U-2OS cell cycle arrest at the G2/M phase (Fig. 2E). Notably, the rate of cell apoptosis in the shCHPF group was significantly enhanced ($P < 0.001$; Fig. 2F), which might be induced through augmenting Bax, Bad, Caspase-3, Caspase-8, CD40L, Fas, IGFBP-4, p27, p53, and SMAC ($P < 0.05$; Fig. 2G, H). On the other hand, we overexpressed CHPF in MNNG/HOS and U-2OS cells so as to further confirm the effects of CHPF on osteosarcoma development. Contrary to the above findings, CHPF overexpression ameliorated osteosarcoma cell proliferation, colony formation, and migration, and mitigated apoptosis (Fig. S2). These
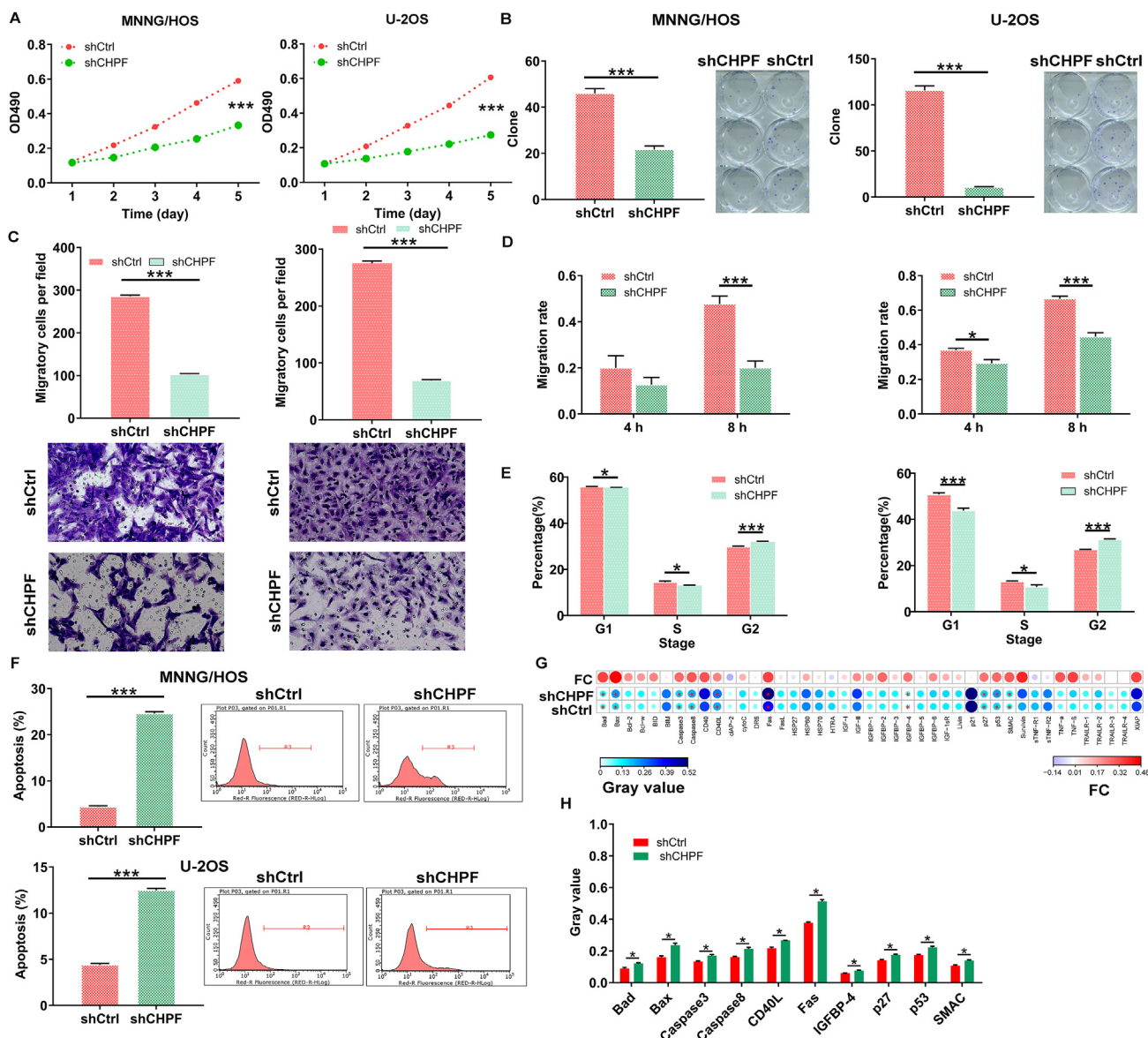
Figure 2 CHPF knockdown inhibited cell proliferation, colony formation and migration, induced cell apoptosis. **(A)** MTT assay was used to detect the effects of CHPF knockdown on cell proliferation of MNNG/HOS and U-2OS cells. **(B)** The abilities of MNNG/HOS and U-2OS cells to form colony after infection were assessed. **(C, D)** The effects of CHPF knockdown on MNNG/HOS and U-2OS cell migration capacities were detected by Transwell assay (C) and wound-healing assay (D). **(E, F)** Flow cytometry was performed to evaluate the effects of CHPF knockdown on cell cycle (E) and apoptosis (F) of MNNG/HOS and U-2OS cells. **(G, H)** The changes in apoptosis-related proteins were analyzed in MNNG/HOS cells following infection by a Human Apoptosis Antibody Array. Protein level was visualized by R studio (G) and presented in gray value (H). The data were expressed as mean ± SD. *$P < 0.05$, ***$P < 0.001$.

results suggested that CHPF plays a tumor-promoting role in osteosarcoma development.

CHPF silencing suppresses the tumorigenic ability of osteosarcoma *in vivo*

To assess the tumorigenic ability of CHPF, MNNG/HOS cells stably infected with shCtrl and shCHPF were subcutaneously injected into mice to establish xenograft models ($n = 10$ per group) (Fig. 3A). Thirty-six days after cell implantation, we observed fewer tumors in the shCHPF group

(Fig. 3B). Additionally, tumors formed from CHPF-depleted MNNG/HOS cells exhibited reduced fluorescence intensity ($P < 0.05$; Fig. 3C). We also monitored the growth indicators of tumors and found that the shCHPF group harbored significantly smaller tumor volume and weight ($P < 0.05$; Fig. 3D, E). Following sacrifice, tumor tissues were harvested for CHPF and Ki-67 protein detection. As expected, CHPF and Ki-67 levels were decreased in tissues from mice injected with shCHPF MNNG/HOS cells (Fig. 3F; Fig. S3A). Taken together, these findings suggested that CHPF depletion caused the tumorigenic ability of osteosarcoma weakened *in vivo*.
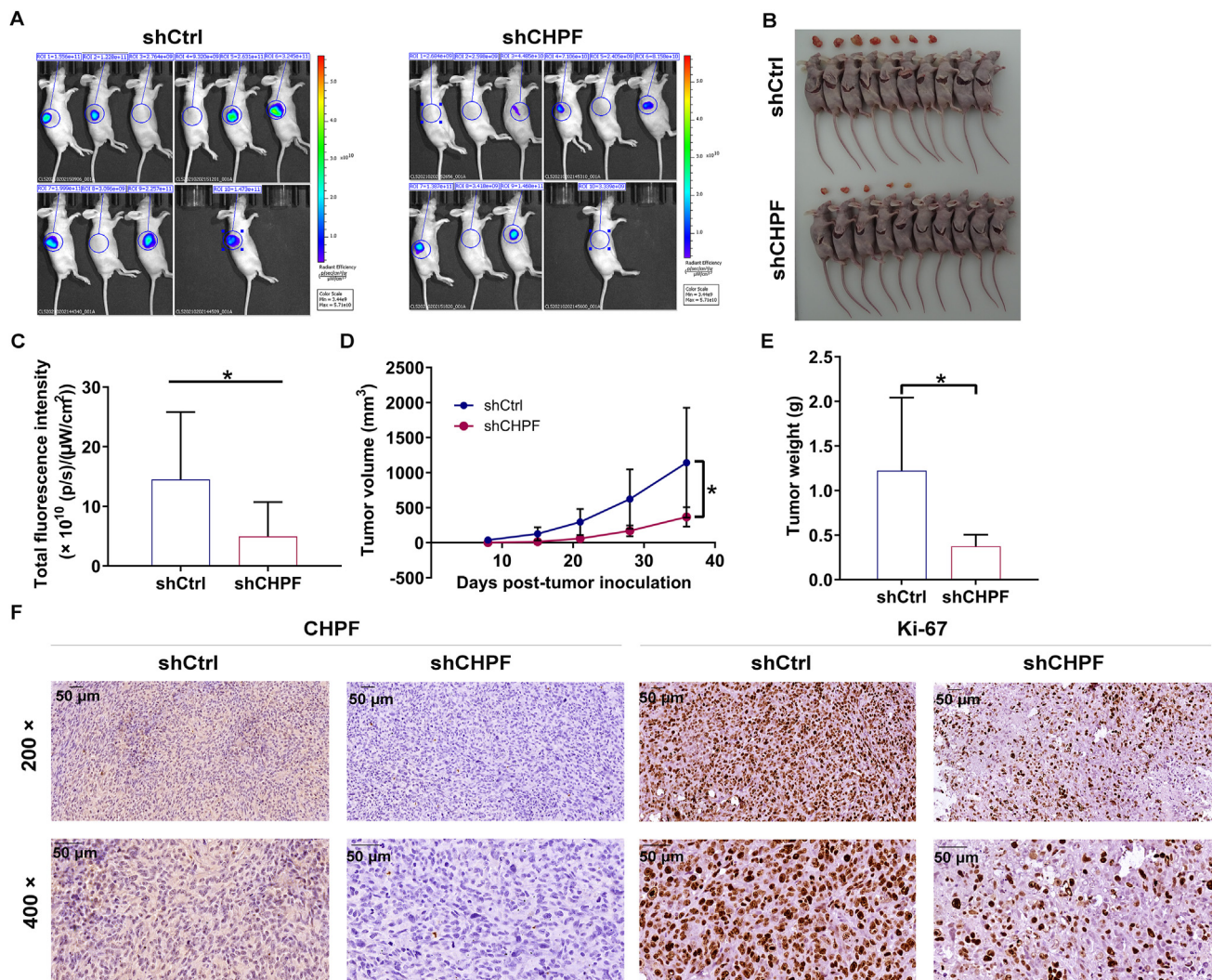
Figure 3 CHPF knockdown inhibited tumor growth of osteosarcoma *in vivo*. **(A)** A nude mice model of CHPF knockdown was constructed. **(B)** The photos of tumors removed from mice models were collected. **(C−E)** The fluorescence (C), volume (D) and weight (E) of xenograft tumors were measured. **(F)** The patterns of CHPF and Ki-67 were detected by IHC analysis in tumor sections from the mice models. The data were expressed as mean $\pm$ SD ($n \geq 3$). *$P < 0.05$.

SKP2 is identified as the target gene of CHPF regulating osteosarcoma

We next executed a PrimeView human gene expression array in CHPF-silenced MNNG/HOS cells to explore the mechanism by which CHPF regulates osteosarcoma. Taking the fold change ≥ 1.3 and *FDR* < 0.05 as a baseline, 5351 differentially expressed genes (DEGs) were obtained (Fig. 4A). These DEGs were subsequently applied to the canonical pathway analysis of Ingenuity pathway analysis (IPA), the results of which showed that Androgen signaling, Sirtuin signaling pathway, Gαq signaling, and Cyclins and cell cycle regulation were blocked upon silencing CHPF (Fig. 4B). The association between these pathways with CHPF was also established through a network analysis of IPA (Fig. 4C). Next, we selected several DEGs with higher fold changes for qRT-PCR detection in MNNG/HOS cells with CHPF downregulation, four of which were selected for Western blot verification. The results demonstrated that the levels of CCND2, CCNE2, RHOU, and SKP2 were

remarkably attenuated at both mRNA and protein levels (Fig. 4D, E; Fig. S3B). We subsequently constructed lentiviral vectors corresponding to CCND2, CCNE2, RHOU, and SKP2 to infect MNNG/HOS cells. The results of Celigo cell counting assay showed that shSKP2 caused a significant reduction in cell proliferation ($P < 0.05$; Fig. 4F). Therefore, we hypothesized that SKP2 is a downstream target of CHPF regulating osteosarcoma and sought to investigate how the loss of CHPF mechanistically affects SKP2 expression at the translational and transcriptional levels. Incidentally, we found that exogenously expressed Flag-CHPF specifically interacted with SKP2, implying that there was a protein interaction between CHPF and SKP2 (Fig. 4G). To further study the mechanism by which CHPF knockdown mediates the reduction in SKP2 protein expression, we treated MNNG/HOS cells with cycloheximide (CHX) to evaluate the half-life of SKP2. The data of Western blotting showed that the inhibition of CHPF accelerated the degradation of SKP2 protein (Fig. 4H), which was partially abolished by adding the proteasome inhibitor MG132

Figure 4   SKP2 was identified as the downstream target of CHPF regulating osteosarcoma. **(A)** PrimeView human gene expression array (3 v 3) was performed to identify differentially expressed genes in MNNG/HOS cells with or without CHPF knockdown. **(B)** The enrichment of the DEGs in canonical signaling pathways was analyzed by IPA. **(C)** The IPA analysis was performed to produce the CHPF-related interaction network. **(D, E)** The expression of several most significantly down-regulated DEGs was further determined via qRT-PCR (D) and Western blotting (E). **(F)** Celigo cell counting assay was performed to detect the inhibition of cell proliferation of MNNG/HOS cells after infecting shCCND2, shCCNE2, shRHOU or shSKP2 corresponding lentiviruses. **(G)** Co-IP assay was used to

(Fig. 4I). This finding implies that CHPF may regulate SKP2 through the ubiquitin-proteasome system (UPS). As it is well-known that the ubiquitination of proteins is usually involved in proteasome-mediated degradation,[16,17] the ubiquitination level of SKP2 was further evaluated. As predicted, CHPF depletion augmented the ubiquitination of SKP2 (Fig. 4J). Thus, we hypothesized that CHPF could regulate osteosarcoma by affecting SKP2 ubiquitination.

Moreover, by analyzing the RNA-seq data collected from the TARGET database, we observed a positive correlation between CHPF level and SKP2 expression (Fig. 4K). More importantly, similar to CHPF, the levels of SKP2 were abundant in both osteosarcoma tissues and cells (Fig. 4L, M; Fig. S3C).

CHPF targets SKP2 to promote osteosarcoma progression

Having identified SKP2 as a downstream gene of CHPF, we sought to verify that CHPF promotes osteosarcoma development through SKP2. Thus, different MNNG/HOS cell models with CHPF overexpression only, SKP2 knockdown only, and CHPF overexpression with SKP2 knockdown were established (Fig. S4). We found that CHPF overexpression significantly increased MNNG/HOS cell proliferation, which was reversed by knocking down SKP2 (Fig. 5A). Additionally, as shown in Figure 5B, a trend toward decreased apoptosis was found following CHPF elevation ($P < 0.01$), which was counteracted by inhibition of SKP2 expression ($P < 0.001$). Furthermore, functional studies of cell migration revealed that when SKP2 was knocked down in CHPF-elevated MNNG/HOS cells, they exhibited a shift toward inhibiting cell migration (Fig. 5C, D). Collectively, these results demonstrated that SKP2 harbored similar effects on the development of osteosarcoma as CHPF, the knockdown of which curbed the promotion effects of CHPF elevation on osteosarcoma.

CHPF promotes osteosarcoma progression through activation of the AKT signaling pathway

In addition to downstream genes, we examined the downstream pathways of CHPF in the regulation of osteosarcoma. Western blot analysis of several cancer-related proteins was performed to evaluate their expression in response to CHPF depletion. The results revealed that the levels of p-AKT, CCND1, CDK1, and PIK3CA were significantly decreased, while the total AKT level was unchanged (Fig. 5E; Fig. S5A). Thus, we considered that the AKT classical signaling pathway may be a downstream pathway of CHPF. The AKT pathway has been shown to be involved in

the progression of various human cancers, including osteosarcoma.[18–20] Therefore, we treated CHPF-depleted MNNG/HOS cells with SC79 (an activator of AKT) to determine whether CHPF-induced osteosarcoma progression was mediated by the AKT pathway. We found that the previously attenuated p-AKT and p-mTOR levels were reversed after SC79 treatment (Fig. 5F; Fig. S5B). Additionally, as shown in Figure 5G, SC79 treatment counteracted the promotion effects of CHPF depletion on cell apoptosis of MNNG/HOS cells. Taken together, these findings suggested that CHPF promotes the development of osteosarcoma by activating the AKT signaling pathway.

Discussion

Osteosarcoma is the most common type of malignant bone tumor worldwide.[1] Since the introduction of chemotherapy and targeted therapy in high-grade osteosarcoma, the prognosis has improved significantly, and two-thirds of patients have achieved long-term survival. However, untreated osteosarcoma continues to develop, with the progression of local and systemic diseases, ultimately causing death within a few months. An increasing number of studies have focused on the pathogenesis of osteosarcoma. It has been reported that LncRNA MEG3 is decreased in osteosarcoma, and it promotes osteosarcoma chemosensitivity by regulating antitumor immunity via the miR-21-5p/p53 pathway and autophagy.[21] Additionally, the mevalonate pathway can promote metastasis of osteosarcoma by activating YAP1 via RhoA.[22] However, the etiology of osteosarcoma remains largely unknown, and further understanding of the molecular mechanism of osteosarcoma development is essential to identify novel therapeutic targets and improve patient outcomes.

CHPF is a 775-amino-acid protein with a molecular mass of approximately 85 kDa.[7–9] Previous studies have revealed the relationship between CHPF and several human cancers. Kalathas et al demonstrated that CHPF plays an important role in the initiation and development of colorectal cancer[13] and laryngeal cancer.[14] Moreover, CHPF has been found to be highly expressed in human glioma tissues and cell lines, indicating that CHPF is a promoter for glioma.[15] However, a detailed understanding of CHPF's mechanisms in the regulation of osteosarcoma is still lacking.

In our study, abundant expression of CHPF was observed in osteosarcoma tissues and cells, which was associated with higher-grade malignancy and pathological stage, suggesting that CHPF is engaged in the tumorigenic activity of osteosarcoma. The oncogenic properties of CHPF were demonstrated in both *in vitro* and *in vivo* assays, highlighting the potential of CHPF as a treatment target for osteosarcoma. In this work, we further investigated the

---

verify whether there was protein interaction between CHPF and SKP2. **(H)** The level of SKP2 protein in MNNG/HOS cells with CHPF depletion was detected following 50 μg/mL CHX treatment for indicated times. **(I)** After MG-132 treatment, the level of SKP2 protein in MNNG/HOS cells with CHPF depletion was examined. **(J)** The lysate of MNNG/HOS cells with CHPF depletion was immunoprecipitated using SKP2 and IgG antibodies, and the Western blotting was performed to examine the ubiquitination of SKP2. **(K)** There was a positive correlation between CHPF level and SKP2 expression through analyzing the RNA-seq data collected from TARGET database. **(L, M)** The protein level of SKP2 in osteosarcoma/normal tissues and the mRNA level of SKP2 in osteosarcoma cell lines were detected via IHC staining (L) and qRT-PCR (M), respectively.
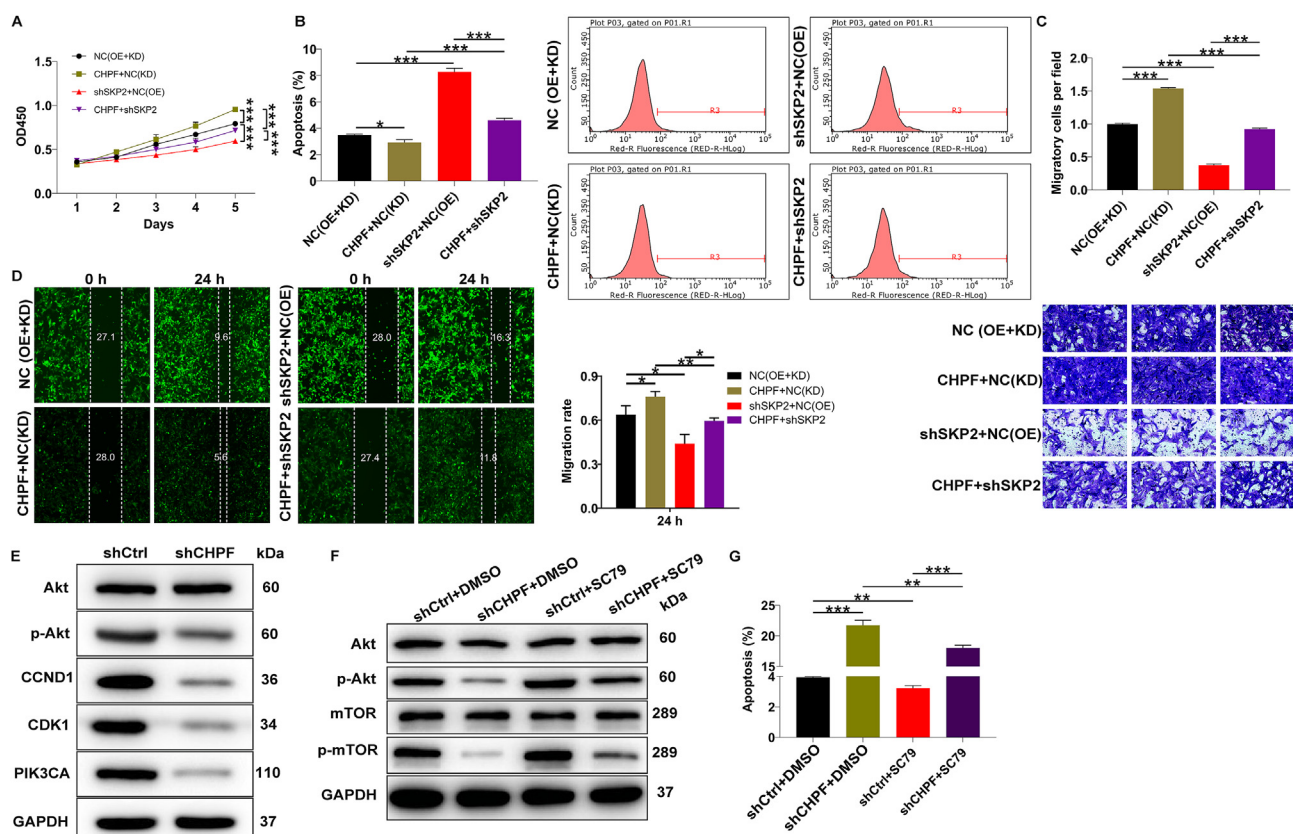
Figure 5 SKP2 knockdown alleviated the promotion of osteosarcoma from CHPF overexpression. **(A)** MTT assay was performed to examine the effects of CHPF overexpression, SKP2 downregulation as well as CHPF overexpression combining with SKP2 down-regulation on MNNG/HOS cell proliferation. **(B)** Flow cytometry was performed to detect the effects of CHPF overexpression, SKP2 downregulation as well as CHPF overexpression combining with SKP2 downregulation on MNNG/HOS cell apoptosis. **(C, D)** The effects of CHPF overexpression, SKP2 downregulation as well as CHPF overexpression combining with SKP2 downregulation on MNNG/HOS cell migration were evaluated by Transwell (C) and wound healing (D) assays. **(E)** The expression of some well-known cancer-associated elements was detected by Western blotting in MNNG/HOS cells after silencing CHPF. **(F)** Western blotting revealed protein expression of AKT, p-AKT, mTOR and p-mTOR in shCtrl or shCHPF infected MNNG/HOS cells treated with or without an AKT activator: SC79. **(G)** Flow cytometry experiment showed the changes in shCtrl or shCHPF infected MNNG/HOS cell apoptosis after treatment with or without SC79. The data were expressed as mean $\pm$ SD ($n \geq 3$). *$P < 0.05$, **$P < 0.01$, ***$P < 0.001$.

downstream genes of CHPF and confirmed that SKP2 had a role in mediating osteosarcoma. SKP2, also known as p45 or FBXL1, is a member of the F-box protein family, which participates in ubiquitination, cell cycle control, and signal transduction in the form of the SKP2-SCF complex (Cul1-Rbx1-SKP1-F-boxSKP2)[23,24]; SKP2 plays a role as a substrate recognition factor.[25] Moreover, SKP2 has been shown to be an oncogene[26] that is overexpressed in lymphoma,[27] prostate cancer,[28] melanoma,[29] nasopharyngeal carcinoma[30] and breast cancer.[31] Here, overexpression of SKP2 was also observed in osteosarcoma tissues and cells. More importantly, our data illustrated that silencing SKP2 could counteract the promotion effects of elevating CHPF on osteosarcoma. We also investigated the mechanism by which CHPF regulates SKP2.

UPS is responsible for the cellular processes associated with protein quality control and homeostasis.[32] Interestingly, the dysregulation of the UPS has been implicated in numerous diseases, including human cancers, in which the components of UPS are frequently mutated or abnormally

expressed.[33] Here, we found that CHPF depletion could accelerate the ubiquitination of SKP2, thereby attenuating SKP2 protein level. Therefore, we proposed that the tumor-promoting potential of CHPF in human osteosarcoma was mediated by counteracting SKP2's ubiquitination.

We also explored the potential downstream pathway of CHPF in the regulation of osteosarcoma. The AKT signaling pathway is one of the most frequently altered pathways in human cancers and plays a critical role in driving tumor initiation and progression.[34] Consequently, the AKT signaling has emerged as an attractive target for cancer therapy, and many drugs that inhibit various pathway components are currently in clinical trials.[35] Published research has shown that the AKT pathway is the most common aberrantly activated pathway in breast cancer.[36] Furthermore, Chen et al[37] demonstrated that progranulin (PGRN) exacerbates the progression of non-small cell lung cancer via the AKT signaling. Furthermore, in osteosarcoma, the AKT pathway is closely related to tumorigenesis and disease progression.[38-40] In this study, we found that

upon knocking down CHPF, p-AKT and p-mTOR levels were downregulated, which was reversed after treatment with SC79. However, SC79 treatment damaged the inhibitory effects of CHPF depletion on the malignant phenotypes of MNNG/HOS cells.

In summary, these findings suggested that CHPF promotes the development of osteosarcoma via targeting SKP2 and activating AKT signaling pathway, which may represent a promising candidate target for treating osteosarcoma. Although our current study provides some important and instructive findings, it still has many limitations. For instance, we did not determine the relationship between CHPF expression and the prognosis of osteosarcoma patients. Additionally, we have not yet determined whether SKP2 regulates osteosarcoma through the AKT pathway. It's well reported that SKP2 is an oncoprotein and promotes AKT activation,[41] we speculated that CHPF increases the expression of SKP2 by inhibiting its ubiquitination, thereby activating the AKT pathway and eventually facilitating osteosarcoma development. More importantly, larger sample sizes are needed to offer a greater degree supporting the role of CHPF in osteosarcoma, which will provide a theoretical basis for new strategies in osteosarcoma diagnosis and treatment.

Author contributions

Yi Shen and Yuanliang Sun designed this research; Jun Li, Dan Peng, and Lele Liao performed the cell and animal experiments; Xia Chen, Zicheng Liu, Chao Yu, and Weiye Zhong conducted the data processing and analysis; and Yi Shen and Jun Li completed the manuscript, which was reviewed by Yuanliang Sun. All of the authors have confirmed the submission of this manuscript.

Conflict of interests

The authors declare that they have no conflict of interests.

Funding

Acknowledgements

Appendix A. Supplementary data

Supplementary data to this article can be found online at https://doi.org/10.1016/j.gendis.2022.06.010.

References

1. Nie Z, Peng H. Osteosarcoma in patients below 25 years of age: an observational study of incidence, metastasis, treatment and outcomes. *Oncol Lett*. 2018;16(5):6502–6514.
2. Zhang B, Zhang Y, Li R, et al. The efficacy and safety comparison of first-line chemotherapeutic agents (high-dose methotrexate, doxorubicin, cisplatin, and ifosfamide) for osteosarcoma: a network meta-analysis. *J Orthop Surg Res*. 2020;15(1):51.
3. Sugahara K, Mikami T, Uyama T, et al. Recent advances in the structural biology of chondroitin sulfate and dermatan sulfate. *Curr Opin Struct Biol*. 2003;13(5):612–620.
4. Perrimon N, Bernfield M. Specificities of heparan sulphate proteoglycans in developmental processes. *Nature*. 2000;404(6779):725–728.
5. Sugumaran G, Katsman M, Sunthankar P, et al. Biosynthesis of chondroitin sulfate. Purification of glucuronosyl transferase II and use of photoaffinity labeling for characterization of the enzyme as an 80-kDa protein. *J Biol Chem*. 1997;272(22):14399–14403.
6. Yada T, Gotoh M, Sato T, et al. Chondroitin sulfate synthase-2. Molecular cloning and characterization of a novel human glycosyltransferase homologous to chondroitin sulfate glucuronyltransferase, which has dual enzymatic activities. *J Biol Chem*. 2003;278(32):30235–30247.
7. Kitagawa H, Izumikawa T, Uyama T, et al. Molecular cloning of a chondroitin polymerizing factor that cooperates with chondroitin synthase for chondroitin polymerization. *J Biol Chem*. 2003;278(26):23666–23671.
8. Kitagawa H, Uyama T, Sugahara K. Molecular cloning and expression of a human chondroitin synthase. *J Biol Chem*. 2001;276(42):38721–38726.
9. Siebert JR, Conta Steencken A, Osterhout DJ. Chondroitin sulfate proteoglycans in the nervous system: inhibitors to repair. *BioMed Res Int*. 2014;2014:845323.
10. Takeuchi J, Sobue M, Sato E, et al. Variation in glycosaminoglycan components of breast tumors. *Cancer Res*. 1976;36(7 PT 1):2133–2139.
11. Pothacharoen P, Najarus S, Settakorn J, et al. Effects of sesamin on the biosynthesis of chondroitin sulfate proteoglycans in human articular chondrocytes in primary culture. *Glycoconj J*. 2014;31(3):221–230.
12. Izumikawa T, Saigoh K, Shimizu J, et al. A chondroitin synthase-1 (ChSy-1) missense mutation in a patient with neuropathy impairs the elongation of chondroitin sulfate chains initiated by chondroitin N-acetylgalactosaminyltransferase-1. *Biochim Biophys Acta*. 2013;1830(10):4806–4812.
13. Kalathas D, Theocharis DA, Bounias D, et al. Chondroitin synthases I, II, III and chondroitin sulfate glucuronyltransferase expression in colorectal cancer. *Mol Med Rep*. 2011;4(2):363–368.
14. Kalathas D, Triantaphyllidou IE, Mastronikolis NS, et al. The chondroitin/dermatan sulfate synthesizing and modifying enzymes in laryngeal cancer: expressional and epigenetic studies. *Head Neck Oncol*. 2010;2:27.
15. Fan YH, Xiao B, Lv SG, et al. Lentivirus-mediated knockdown of chondroitin polymerizing factor inhibits glioma cell growth *in vitro*. *Oncol Rep*. 2017;38(2):1149–1155.
16. Inobe T, Matouschek A. Paradigms of protein degradation by the proteasome. *Curr Opin Struct Biol*. 2014;24:156–164.
17. Kang DC, Gao XQ, Ge QF, et al. Effects of ultrasound on the beef structure and water distribution during curing through protein degradation and modification. *Ultrason Sonochem*. 2017;38:317–325.
18. Zhang Y, Weng Q, Han J, et al. Alantolactone suppresses human osteosarcoma through the PI3K/AKT signaling pathway. *Mol Med Rep*. 2020;21(2):675–684.
19. Li X, Huang Q, Wang S, et al. HER4 promotes the growth and metastasis of osteosarcoma via the PI3K/AKT pathway. *Acta Biochim Biophys Sin*. 2020;52(4):345–362.
20. Vara JÁF, Casado E, de Castro J, et al. PI3K/Akt signalling pathway and cancer. *Cancer Treat Rev*. 2004;30(2):193–204.

21. Huang X, Zhang W, Pu F, et al. LncRNA MEG3 promotes che-mosensitivity of osteosarcoma by regulating antitumor immu-nity via miR-21-5p/p53 pathway and autophagy. *Genes Dis*. 2023;10(2):531—541.

22. Du X, Ou Y, Zhang M, et al. The mevalonate pathway promotes the metastasis of osteosarcoma by regulating YAP1 activity via RhoA. *Genes Dis*. 2022;9(3):741—752.

23. Bai C, Sen P, Hofmann K, et al. SKP1 connects cell cycle reg-ulators to the ubiquitin proteolysis machinery through a novel motif, the F-box. *Cell*. 1996;86(2):263—274.

24. Craig KL, Tyers M. The F-box: a new motif for ubiquitin dependent proteolysis in cell cycle regulation and signal transduction. *Prog Biophys Mol Biol*. 1999;72(3):299—328.

25. Nakayama KI, Nakayama K. Regulation of the cell cycle by SCF-type ubiquitin ligases. *Semin Cell Dev Biol*. 2005;16(3):323—333.

26. Wang H, Cui J, Bauzon F, et al. A comparison between Skp2 and FOXO1 for their cytoplasmic localization by Akt1. *Cell Cycle*. 2010;9(5):1021—1022.

27. Seki R, Okamura T, Koga H, et al. Prognostic significance of the F-box protein Skp2 expression in diffuse large B-cell lym-phoma. *Am J Hematol*. 2003;73(4):230—235.

28. Wang Z, Gao D, Fukushima H, et al. Skp2: a novel potential therapeutic target for prostate cancer. *Biochim Biophys Acta*. 2012;1825(1):11—17.

29. Rose AE, Wang G, Hanniford D, et al. Clinical relevance of SKP2 alterations in metastatic melanoma. *Pigment Cell Melanoma Res*. 2011;24(1):197—206.

30. Fang FM, Chien CY, Li CF, et al. Effect of S-phase kinase-associated protein 2 expression on distant metastasis and survival in nasopharyngeal carcinoma patients. *Int J Radiat Oncol*. 2009;73(1):202—207.

31. Radke S, Pirkmaier A, Germain D. Differential expression of the F-box proteins Skp2 and Skp2B in breast cancer. *Oncogene*. 2005;24(21):3448—3458.

32. Nandi D, Tahiliani P, Kumar A, et al. The ubiquitin-proteasome system. *J Biosci*. 2006;31(1):137—155.

33. Nakamura N. Ubiquitin system. *Int J Mol Sci*. 2018;19(4):1080.

34. Hanahan D, Weinberg RA. Hallmarks of cancer: the next gen-eration. *Cell*. 2011;144(5):646—674.

35. Engelman JA. Targeting PI3K signalling in cancer: opportunities, challenges and limitations. *Nat Rev Cancer*. 2009;9(8):550—562.

36. Ellis H, Ma CX. PI3K inhibitors in breast cancer therapy. *Curr Oncol Rep*. 2019;21(12):110.

37. Chen S, Bie M, Wang X, et al. PGRN exacerbates the progression of non-small cell lung cancer via PI3K/AKT/Bcl-2 antiapoptotic signaling. *Genes Dis*. 2021;9(6):1650—1661.

38. Naef V, De Sarlo M, Testa G, et al. The stemness gene Mex3A is a key regulator of neuroblast proliferation during neuro-genesis. *Front Cell Dev Biol*. 2020;8:549533.

39. Liu G, Yuan D, Sun P, et al. LINC00968 functions as an oncogene in osteosarcoma by activating the PI3K/AKT/mTOR signaling. *J Cell Physiol*. 2018;233(11):8639—8647.

40. Liu B, Xu L, Dai EN, et al. Anti-tumoral potential of MDA19 in human osteosarcoma via suppressing PI3K/Akt/mTOR signaling pathway. *Biosci Rep*. 2018;38(6):BSR20181501.

41. Han F, Li CF, Cai Z, et al. The critical role of AMPK in driving Akt activation under stress, tumorigenesis and drug resistance. *Nat Commun*. 2018;9(1):4728.